

Electronic transport coefficients from density functional theory across the plasma plane

Martin French ¹, Gerd Röpke ¹, Maximilian Schörner ¹, Mandy Bethkenhagen ^{1,2},
Michael P. Desjarlais,³ and Ronald Redmer ¹

¹Universität Rostock, Institut für Physik, Albert-Einstein-Str. 23-24, D-18059 Rostock, Germany

²École Normale Supérieure de Lyon, Université Lyon 1, Laboratoire de Géologie de Lyon, CNRS UMR 5276, 69364 Lyon Cedex 07, France

³Sandia National Laboratories, Albuquerque, New Mexico 87185, USA



(Received 1 March 2022; accepted 18 May 2022; published 10 June 2022)

We investigate the thermopower and Lorenz number of hydrogen with Kohn-Sham density functional theory (DFT) across the plasma plane toward the near-classical limit, i.e., weakly degenerate and weakly coupled states. Our results are in concordance with certain limiting values for the Lorentz plasma, a model system which only considers electron-ion scattering. Thereby, we clearly show that the widely used method of calculating transport properties via the Kubo-Greenwood (KG) formalism does not capture electron-electron scattering processes. Our discussion also addresses the inadequateness of assuming a Drude-like frequency behavior for the conductivity of nondegenerate plasmas by revisiting the relaxation time approximation within kinetic theory.

DOI: [10.1103/PhysRevE.105.065204](https://doi.org/10.1103/PhysRevE.105.065204)

I. INTRODUCTION

Besides the equation of state and the optical properties, the transport coefficients are important quantities to characterize the state of metals and plasmas. The electrical and thermal conductivity, $\sigma(n, T)$ and $\lambda(n, T)$, as well as the thermopower $\alpha(n, T)$ and Lorenz number (named after Ludvig V. Lorenz [1]) $L(n, T)$ depend in general on the particle density n and temperature T but have well-known values for fully degenerate plasmas according to the Ziman theory [2] and in the nondegenerate limit as derived in the seminal work of Spitzer and Härm [3].

Solving fundamental geo- and astrophysical questions on structure, evolution, and magnetic field generation in stars and planets relies on accurate knowledge of σ and λ of stellar and planetary matter [4–9]. The experimental determination of transport properties for plasmas and metals at such high temperatures is very challenging, and a large part of the research in the field is carried out via theoretical and computational methods [10].

The computation of transport coefficients is possible via kinetic theory [11–15], which was introduced originally for low-density systems. Calculations for dense plasmas have to address fundamental problems, e.g., dynamical screening and strong collisions between electrons and ions, the influence of the ionic structure during the collisions (dynamic ion-ion structure factor), and partial ionization (bound states) [16–18]. The fluctuation-dissipation theorem [19] and a Hamiltonian-based linear response description [20] have been invented to relate transport coefficients to equilibrium correlation functions. A generalized linear response theory [21,22] makes this approach practically more applicable, for instance for the evaluation of the equilibrium correlation functions by perturbation theory and establishing the link to kinetic theory [23]. Alternatively, density functional theory (DFT) can be applied

to calculate transport coefficients via the Kubo-Greenwood (KG) formalism [20,24,25]. DFT-MD simulations, which combine the quantum treatment of electrons via density functional theory with the molecular-dynamical (MD) solution of the ionic motion, allow us to treat strongly coupled Coulomb systems beyond perturbation theory, e.g., dense nonideal plasmas up to condensed matter densities, the so-called warm dense matter. The effectiveness of the KG approach, which uses the Kohn-Sham orbitals and energies from DFT, has been demonstrated in particular for dense plasmas and warm dense matter [26–35].

Although the DFT-based approach to calculate transport coefficients in dense plasmas via the KG formalism is very successful, a fundamental question is still open: whether or not the influence of electron-electron (e-e) collisions is properly included. While e-e *correlations* are accounted for by the exchange-correlation energy functional in some approximation to obtain optimal electronic orbitals, it is not clear whether the exact calculation of e-e *collisions* can be performed within a single-particle description without the explicit treatment of two-particle Coulomb interactions. This problem has received increasing attention recently [36–39] and can be checked best in the low-density and high-temperature region of hydrogen plasmas, where exchange and correlation energies become irrelevant and exact results for the transport coefficients are available from the Spitzer theory [3]. Unfortunately, this is just the region where Kohn-Sham-DFT becomes computationally demanding because high temperatures and low densities require huge simulation cells and a large number of bands, so that it is very challenging to converge the calculations. For instance, Desjarlais *et al.* [37] applied a Drude-like fit to the very low-frequency behavior of the transport coefficients. From these extrapolated values, it was concluded that the electrical conductivity agreed with quantum Lenard-Balescu (QLB) [40–43] results that include

e-e scattering, whereas the thermal conductivity was too high by a factor of about two. While these results ruled out for the first time explicit e-e scattering in the DFT calculations, the agreement with the QLB results suggested that a reduction in the electrical conductivity analogous to that found in Spitzer theory due to e-e interactions was present. Shaffer and Starrett [38] supported this argument in their discussion. In contrast, a recent analysis of DFT-MD data within a virial expansion of the electrical conductivity [39] hinted toward e-e collisions not being correctly accounted for at any level.

Here we re-examine the DFT calculations from Ref. [37] and show that they were, unfortunately, not sufficiently converged and that the agreement with QLB results that included e-e scattering [37] was accidental. Although our computational capabilities to converge DFT transport properties at the conditions chosen by Desjarlais *et al.* [37] are still insufficient, we give a clear answer to the question, whether or not e-e scattering is correctly included in the KG formalism, via an alternative route which utilizes the thermopower and Lorenz number calculated at less extreme plasma conditions. Related to the DFT calculations, we also address the inadequacy of assuming a Drude-like frequency dependence in nondegenerate plasmas in a special section about the relaxation time approximation.

In short, this paper shows the first fully converged and convincing results that a DFT-based evaluation of the KG formula does not include exact contributions from e-e collisions. To make this inference, we have performed extensive DFT calculations for hydrogen plasma along a special path across the density-temperature plane. We find that the asymptotic behavior of the calculated transport coefficients converges clearly to the values of the Lorentz plasma, which is a model system (named after Hendrik A. Lorentz [11,44]) *without* e-e collisions, where only the electron-ion (e-i) interactions are considered, usually described by an effective (screened) potential.

II. PLASMA PARAMETERS

The state of a hydrogen plasma can be generally characterized with two dimensionless parameters [45] that depend on electron density n_e and temperature T . The first is the coupling parameter, which relates the average Coulomb interaction energy to the thermal energy,

$$\Gamma = \frac{e^2}{4\pi\epsilon_0 k_B T} \left(\frac{4\pi n_e}{3} \right)^{1/3}, \quad (1)$$

where e is the elementary charge, ϵ_0 is the vacuum permittivity, and k_B is Boltzmann's constant. Second, the degeneracy parameter describes the importance of quantum effects (degeneracy, Pauli blocking, etc.) and is given by

$$\Theta = \frac{8\pi\epsilon_0 k_B T}{e^2 a_B} \left(\frac{1}{3\pi^2 n_e} \right)^{2/3}, \quad (2)$$

where a_B is the Bohr radius.

A path perpendicular to the $\Gamma = 1$ and $\Theta = 1$ lines, which rise on geometric average with a power of $T \sim n_e^{1/2}$ in the

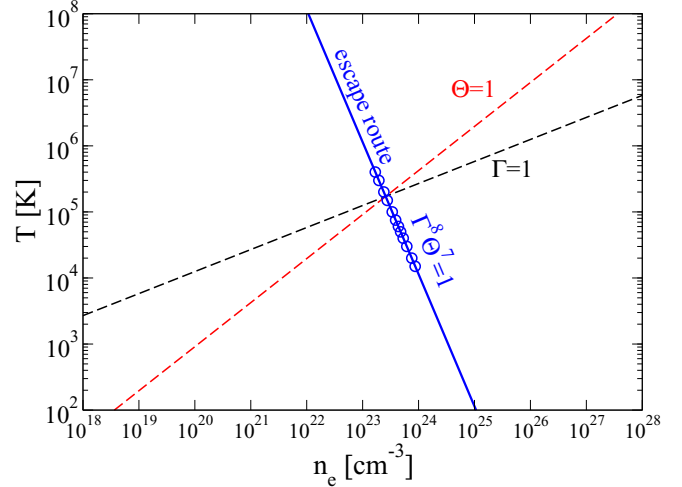


FIG. 1. Density-temperature plane of H plasma with the relevant lines: $\Theta = 1$, $\Gamma = 1$, and $\Gamma^8 \Theta^7 = 1$. Blue circles indicate the conditions chosen for our calculations.

plasma plane, can be defined as follows:

$$T = \left(\frac{4}{9\pi} \right)^{14/3} \left(\frac{3}{4\pi} \right)^2 \left(\frac{2}{a_B} \right)^7 \frac{e^2}{4\pi\epsilon_0 k_B n_e^2}, \quad (3)$$

or equivalently by $\Gamma^8 \Theta^7 = 1$. We may call this path an escape route from correlation and quantum effects because it represents the shortest route from the highly degenerate ($\Theta \ll 1$) and strongly coupled ($\Gamma \gg 1$) region to the nondegenerate ($\Theta \gg 1$) and weakly coupled ($\Gamma \ll 1$) conditions, anchored at $\Gamma = \Theta = 1$; see Fig. 1.

Following this route allows us to efficiently reach conditions for which certain limiting laws for the transport coefficients of plasmas are known. Our main DFT calculations were run along this path between 15 000 K and 1.46 g/cm³ up to 400 000 K and 0.2826 g/cm³ and closely approached characteristic limiting cases at both ends.

III. RELAXATION TIME APPROXIMATION

Before discussing our DFT calculations, we describe a simpler and well understood approach to calculate electronic transport properties of plasmas, which will be used for various comparisons. This model considers a Lorentz plasma, where electrons scatter only at ions via a statically screened Coulomb potential and all particles are uncorrelated. It is derived by solving the Boltzmann equation within the relaxation time approximation (RTA) [11], which was done, e.g., by Lee and More [46] and can be evaluated for arbitrary degeneracy.

When assuming frequency-dependent perturbations $\sim \exp(i\omega t)$ by an electrical field $\mathbf{E}(\omega)$ and a temperature gradient $\nabla T(\omega)$ at constant pressure, the following nonequilibrium distribution function for the plasma electrons is derived:

$$f(\mathbf{v}) = f_0 + \frac{\tau}{1 + i\omega\tau} \frac{\partial f_0}{\partial E} \mathbf{v} \cdot \left[e\mathbf{E} + \left(\frac{E - h_e}{T} \right) \nabla T \right], \quad (4)$$

where h_e is the enthalpy per electron, \mathbf{v} the velocity, $\tau = \tau(E)$ the relaxation time, and $f_0(E)$ is the Fermi distribution

function:

$$f_0(E) = \frac{1}{z^{-1} \exp(E/k_B T) + 1}. \quad (5)$$

The Fermi function depends on the kinetic energy $E = m_e \mathbf{v}^2/2$ and fugacity $z = \exp(\mu_e/k_B T)$, where m_e is the mass and μ_e is the chemical potential of the electrons.

A. Zero-frequency limit

After calculating the expectation values of electrical current \mathbf{j} and generalized heat current \mathbf{j}'_Q at $\omega = 0$,

$$\mathbf{j} = -\frac{2em_e^3}{(2\pi\hbar)^3} \int d^3\mathbf{v} \mathbf{v} f(\mathbf{v}), \quad (6)$$

$$\mathbf{j}'_Q = \frac{2m_e^3}{(2\pi\hbar)^3} \int d^3\mathbf{v} \mathbf{v} \left(\frac{m_e \mathbf{v}^2}{2} - h_e \right) f(\mathbf{v}), \quad (7)$$

the following set of Onsager coefficients is obtained, which can be written as integrals over the energy:

$$K_n = \frac{-8(-e)^{2-n}}{3\pi^{1/2} m_e \lambda_e^3 (k_B T)^{3/2}} \int_0^\infty dE E^{n+3/2} \tau(E) \frac{\partial f_0}{\partial E}, \quad (8)$$

where $\lambda_e = \hbar\sqrt{2\pi/m_e k_B T}$ is the thermal wavelength. When assuming only e-i scattering at a screened Coulomb potential, the relaxation time in first Born approximation reads [47–49]

$$\tau(E) = \frac{2^{7/2} \pi \varepsilon_0^2 m_e^{1/2} E^{3/2}}{n_i Z_i^2 e^4 \ln \Lambda(E)}, \quad (9)$$

where n_i and $Z_i = 1$ are density and charge state of the ions, respectively. Due to its weak energy dependence, the Coulomb logarithm $\ln \Lambda(E)$ may be pulled out of the integration and later evaluated at a mean value, which then leads to the following expression:

$$K_n = \frac{2^5 \varepsilon_0^2 m_e (k_B T)^3}{3\pi \hbar^3 n_i Z_i^2 e^2} \left(\frac{k_B T}{-e} \right)^n \frac{\Gamma_{n+4} F_{n+2}(z)}{\ln \Lambda(z)}, \quad (10)$$

where the Fermi integrals are defined as

$$F_j(z) = \frac{1}{\Gamma_{j+1}} \int_0^\infty dx \frac{x^j}{z^{-1} \exp(x) + 1}, \quad (11)$$

with Euler's gamma function Γ_{j+1} .

Here we deviate from the original Lee-More model and use the following formula for the statically screened Coulomb logarithm [48–50]:

$$\ln \Lambda = \frac{1}{2} \left[\ln(1+b) - \frac{b}{1+b} \right], \quad (12)$$

with the following argument:

$$b(z) = \frac{8m_e \tilde{E}(z)}{\hbar^2 \kappa_e^2(z)} = \frac{6m_e (k_B T)^2 \varepsilon_0 \lambda_e^3 F_{1/2}(z)}{\hbar^2 e^2 F_{-1/2}^2(z)}. \quad (13)$$

The equation above follows from the screening parameter of a Lorentz plasma [17]:

$$\kappa_e^2(z) = \frac{2e^2}{\varepsilon_0 \lambda_e^3 k_B T} F_{-1/2}(z), \quad (14)$$

and from calculating the mean energy of the *scattering* electrons as

$$\tilde{E}(z) = \frac{\int dE E^{1/2} E \frac{\partial f_0}{\partial E}}{\int dE E^{1/2} \frac{\partial f_0}{\partial E}} = \frac{3}{2} k_B T \frac{F_{1/2}(z)}{F_{-1/2}(z)}, \quad (15)$$

which gives $\tilde{E} = 3k_B T/2$ in the nondegenerate limit and $\tilde{E} = E_F$, which is the Fermi energy, for complete degeneracy.

In summary, all transport coefficients of interest can be calculated within this RTA model by evaluating a set of six Fermi integrals and using an inversion formula for the fugacity, see, e.g., Ref. [18]. In particular, the electrical conductivity is given by

$$\sigma = K_0 = \frac{2^6 \varepsilon_0^2 m_e (k_B T)^3}{\pi \hbar^3 n_i Z_i^2 e^2} \frac{F_2(z)}{\ln \Lambda(z)}. \quad (16)$$

With the ideal enthalpy per electron,

$$h_e = \frac{5}{2} k_B T \frac{F_{3/2}(z)}{F_{1/2}(z)}, \quad (17)$$

the thermopower coefficient can be written as

$$a = -\frac{e}{k_B} \alpha_e = \frac{-e K_1}{k_B T K_0} - \frac{h_e}{k_B T} = 4 \frac{F_3(z)}{F_2(z)} - \frac{5}{2} \frac{F_{3/2}(z)}{F_{1/2}(z)}. \quad (18)$$

Finally, the Lorenz number is

$$L = \left(\frac{e}{k_B T} \right)^2 \left(\frac{K_2}{K_0} - \frac{K_1^2}{K_0^2} \right) = 20 \frac{F_4(z)}{F_2(z)} - 16 \frac{F_3^2(z)}{F_2^2(z)}. \quad (19)$$

Here the Wiedemann-Franz law, $L = \pi^2/3$, follows directly from the Sommerfeld expansion of Fermi integrals. Expressions for the nondegenerate limits are easily obtained, since all $F_j(z) \approx z = n_e \lambda_e^3/2$ there, e.g., we immediately find the numbers $a = 1.5$ and $L = 4$.

B. Frequency-dependent coefficients

The frequency-dependent coefficients are derived in the same way as Eq. (8). Their real parts then read

$$K_n(\omega) = \frac{-8(-e)^{2-n}}{3\pi^{1/2} m_e \lambda_e^3 (k_B T)^{3/2}} \int_0^\infty dE \frac{E^{n+3/2} \tau(E)}{1 + \omega^2 \tau^2(E)} \frac{\partial f_0}{\partial E}. \quad (20)$$

An analytical integration shows that the coefficient $K_0(\omega) = \sigma(\omega)$ fulfills the sum rule [37],

$$\frac{2m_e}{\pi e^2} \int_0^\infty d\omega \sigma(\omega) = \frac{2}{\lambda_e^3} F_{1/2}(z) = n_e, \quad (21)$$

for any relaxation time $\tau(E)$ if the thermodynamics of the electron gas is ideal.

Equation (20) can be integrated numerically using the relaxation time (9). To remain fully consistent with the previous subsection, we keep the Coulomb logarithm constant here, too. Note that a Drude behavior of the coefficients $K_n(\omega) \sim (1 + \omega^2 \tau^2)^{-1}$ is found only in the fully degenerate limit, where $\tau = \tau(E_F)$. For weakly degenerate electrons, the $\sim E^{3/2}$ proportionality of the relaxation time generates significantly different frequency dependencies of the $K_n(\omega)$.

IV. DFT CALCULATIONS

We use a combination of density functional theory (DFT) [51,52] and molecular dynamics (MD) to simulate the ion dynamics in our H plasma using the VASP code [53–55], generating ionic configurations for subsequent calculations of transport coefficients. In these DFT-MD simulations, we treat exchange and correlation effects with the Perdew, Burke, Ernzerhof (PBE) approximation [56] and use a PAW pseudopotential (labeled PAW H_h_GW) [57,58] with a plane-wave energy cutoff of 1200 eV and the Baldereschi mean-value point [59]. We simulate either 64, 128, or 256 atoms for several 1000 time steps with a length of 0.1 fs at constant temperatures regulated with a Nosé-Hoover thermostat [60,61]. This is done for temperatures between 15 000 and 75 000 K. The pair correlation functions indicate that the ionic structures become increasingly uncorrelated as temperature rises and density decreases; see Appendix A for more details. We therefore use the same ionic configurations from the DFT-MD simulations made at 75 000 K for all calculations of transport coefficients at higher temperatures and only rescale the box sizes to have them match the required smaller densities. This simplification may introduce inaccuracies in the region of intermediate coupling. Nevertheless, it warrants the emergence of configurations of uncorrelated, distant ions toward sufficiently low density and, thus, achieve consistency with the assumptions made in the derivation of the Lorentz and Spitzer limiting values we aim to compare with.

The electronic transport coefficients are then calculated with static DFT calculations using 5–10 ionic configurations from each DFT-MD run and sufficiently large \mathbf{k} -point sets [59,62] to reach convergence. Here we exclusively use the bare Coulomb potential with a cutoff energy of 2000 eV for the electron-ion interactions. The necessary number of bands was determined for each individual density and temperature with systematic convergence tests. It increases drastically with the temperature along the $\Gamma^8\Theta^7 = 1$ line. For example, 120 bands per atom were found to be sufficient at 300 000 K ($\Gamma = 0.52$ and $\Theta = 2.1$). The following expressions for the frequency-dependent Onsager coefficients [25] are evaluated:

$$L_n(\omega) = \frac{2\pi(-e)^{2-n}}{3V\omega} \sum_{\mathbf{k}\nu\mu} |\langle \mathbf{k}\nu | \hat{\mathbf{v}} | \mathbf{k}\mu \rangle|^2 (f_{\mathbf{k}\nu} - f_{\mathbf{k}\mu}) \times \left(\frac{E_{\mathbf{k}\mu} + E_{\mathbf{k}\nu}}{2} - h_e \right)^n \delta(E_{\mathbf{k}\mu} - E_{\mathbf{k}\nu} - \hbar\omega), \quad (22)$$

where ω is the frequency, V the volume of the simulation box, $E_{\mathbf{k}\mu}$ and $f_{\mathbf{k}\mu}$ are the energy eigenvalue and Fermi occupation number of the Bloch state $|\mathbf{k}\mu\rangle$ calculated from DFT, and $\langle \mathbf{k}\nu | \hat{\mathbf{v}} | \mathbf{k}\mu \rangle$ are matrix elements with the velocity operator taken from the optical routines of VASP [63]. The enthalpy per electron $h_e = \mu_e + Ts_e$ is calculated from the chemical potential μ_e and entropy per electron s_e that are derived self-consistently in the DFT. Due to the discrete spectrum of eigenvalues caused by the periodic boundary conditions of the simulation box, it is necessary to broaden the delta function to a small, finite width, which is done here with a Gaussian function.

The static electrical conductivity is the limit of $L_0(\omega)$ at zero frequency, also known as the Kubo-Greenwood

formula [20,24]:

$$\sigma = \lim_{\omega \rightarrow 0} L_0(\omega), \quad (23)$$

while the thermal conductivity can be calculated via

$$\lambda = \frac{1}{T} \lim_{\omega \rightarrow 0} \left(L_2(\omega) - \frac{L_1^2(\omega)}{L_0(\omega)} \right). \quad (24)$$

In addition, we can directly obtain the thermopower coefficient:

$$a = -\frac{e}{k_B} \alpha = -\frac{e}{k_B T} \lim_{\omega \rightarrow 0} \frac{L_1(\omega)}{L_0(\omega)}, \quad (25)$$

and the Lorenz number:

$$L = \left(\frac{e}{k_B T} \right)^2 \lim_{\omega \rightarrow 0} \left[\frac{L_2(\omega)}{L_0(\omega)} - \frac{L_1^2(\omega)}{L_0^2(\omega)} \right]. \quad (26)$$

The corresponding phenomenological equations read [64]:

$$\mathbf{j} = L_0 \mathbf{E} - \frac{L_1}{T} \nabla T = \sigma \mathbf{E} - \sigma \alpha \nabla T, \quad (27)$$

$$\mathbf{j}'_Q = L_1 \mathbf{E} - \frac{L_2}{T} \nabla T = T \sigma \alpha \mathbf{E} - (\lambda - T \sigma \alpha^2) \nabla T. \quad (28)$$

Note that the coefficients K_n used in the RTA model in Sec. III differ from the coefficients L_n of the KG formalism by terms proportional to h_e/e :

$$L_0 = K_0, \quad (29)$$

$$L_1 = K_1 + \frac{h_e}{e} K_0, \quad (30)$$

$$L_2 = K_2 + \frac{2h_e}{e} K_1 + \frac{h_e^2}{e^2} K_0. \quad (31)$$

Because Eqs. (23)–(26) cannot be evaluated directly at $\omega = 0$, extracting their converged DC limits is challenging, especially at high temperatures due to the large number of partially occupied bands that contribute to the summations in the small- ω region. Especially, having a higher index n in the coefficients L_n results in stronger weighting of summands with higher eigenenergies $E_{\mathbf{k}\nu}$. This causes the quantities from Eqs. (23)–(26) to show different convergence behaviors at small ω . For all numerical values presented here, we have ensured that sufficient convergence has been reached to guarantee unbiased extrapolations (here using linear functions) to obtain the DC numbers.

The quantities most challenging to converge at high T are the thermal conductivity (24) and the electrical conductivity (23), because they approach their ordinates with a very steep slope. These calculations require very large particle numbers to resolve the low-frequency region sufficiently well to guarantee precise extrapolations to the DC limit. Desjarlais *et al.* [37] assumed that the conductivity shows Drude-like frequency dependence at low frequency and performed extrapolations to $\omega = 0$ accordingly. A global Drude-like frequency dependence requires that the dynamics of all electrons contributing to the conductivity is determined by a single relaxation time τ [50]. This case holds approximately for degenerate electrons ($\Theta \ll 1$), where Pauli blocking allows scattering processes only for electrons near the Fermi level. But in general, the relaxation time depends on the velocity v

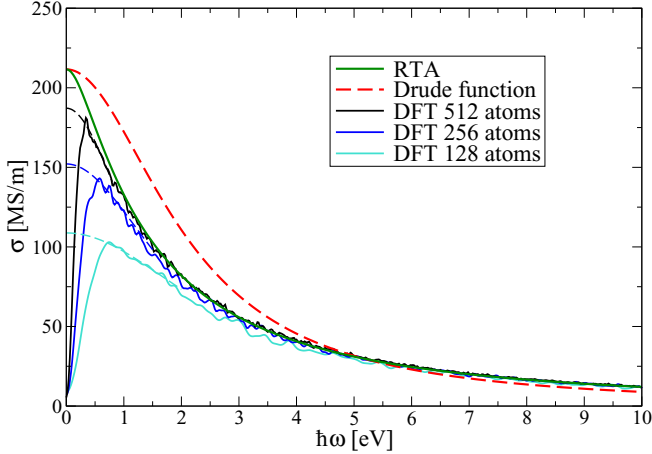


FIG. 2. Frequency-dependent electrical conductivity of hydrogen at 40 g/cm^3 and 500 eV from DFT in comparison with the results from RTA, Eq. (20). Thin dashed lines indicate extrapolations with Drude functions, $\sigma = \sigma_0/(1 + \omega^2\tau^2)$, fitted to the DFT data at frequency ranges between 0.5 and 2 eV . For comparison a Drude function scaled to match the zero-frequency value of the RTA and, simultaneously, fulfill the sum rule (21) is also shown.

of the incident electron, e.g., assuming electron-ion scattering in first Born approximation as in Eq. (9), we have $\tau \sim v^3/\ln \Lambda(v)$. Thus, the frequency dependence of the conductivity cannot be expected to globally match with a Drude-like form at high temperatures and this, in turn, will add uncertainty when employing low-frequency extrapolations to the DC limit. The following section illustrates this problem in more detail by re-examining an example from the work of Desjarlais *et al.* [37] who investigated hydrogen at very high density and temperature.

V. RE-EXAMINATION OF CALCULATIONS FROM DESJARLAIS ET AL. (2017)

We have independently revisited the DFT calculations by Desjarlais *et al.* [37] at $k_B T = 500 \text{ eV}$ and 40 g/cm^3 ($\Gamma = 0.13$) by performing new DFT-MD simulations with 128, 256, and 512 hydrogen atoms. The simulations were run with a time step of 0.003 fs , 25 bands per atom, and a plane-wave cutoff energy of 5000 eV . The electrical conductivity was then calculated from several ionic configurations with 30 bands per atom and a plane-wave cutoff energy of 8000 eV . The Baldereschi \mathbf{k} point [59] was used in all calculations. Results are displayed in Fig. 2.

It is clearly seen that the DFT conductivities are missing essential contributions at low frequency the fewer particles are considered, thus, even the calculations with 512 atoms are likely still underconverged. At sufficiently high frequency, all DFT results merge with the RTA curve, which is derived independently from the DFT and whose shape is determined by the energy dependence of the relaxation time (9). This convinces us to conclude that, at these weakly coupled conditions, the RTA indicates the correct zero-frequency limit that DFT would produce if convergence could be reached.

Both the RTA and Drude models have a quadratic dependence on frequency for very low frequency, but have

differing higher-order dependence. The Drude-like extrapolation to zero frequency will introduce inaccuracy in the zero frequency limit, relative to the RTA functional form, when convergence with respect to particle number is insufficient. In Ref. [37], the zero-frequency limit was derived from simulations with 256 atoms, the limit of what was computationally feasible at the time. The zero frequency limit was obtained through an extrapolation with a Drude function fitted to data between ~ 0.5 and 1 eV . These circumstances lead to an underestimation of the electrical conductivity and, consequently, to a qualitatively different interpretation of results because of an accidental concordance with Lenard-Balescu calculations. Given that the other two conditions from Ref. [37] at 700 and 900 eV are even more challenging to converge, those results for the electrical and thermal conductivity would also be expected to be unconverged with respect to particle number.

Our present inability to converge the DC electrical conductivity at $k_B T = 500 \text{ eV}$ and 40 g/cm^3 requires us to seek alternative options to solve our scientific question. The first adjustment is reducing the density and temperature to less extreme conditions by following the escape route $\Gamma^8\Theta^7 = 1$. Second, instead of founding our reasoning on the electrical and thermal conductivity we will utilize the thermopower and Lorenz number instead. These quantities require less extreme particle numbers for the determination of their DC values as is explained in the next section.

VI. THERMOPOWER AND LORENZ NUMBER ALONG THE ESCAPE ROUTE

While the considerations explained in the preceding section, in principle, also apply to the thermopower coefficient (25) and the Lorenz number (26), these quantities are a lot less prone to the convergence issues discussed. This is likely explained by Eqs. (25) and (26) being ratios of Onsager coefficients (22) by definition, which results in a partial compensation of the leading terms that determine the slopes in the L_n at small frequencies. Consequently, these functions approach their ordinates much less steeply. Their DC values can be found much more easily by standard means of comparing results obtained with different particle numbers and extrapolating the physically relevant section of the curves across the regions of artificial drops (in L_n) or divergences (in certain ratios of different L_n) close to $\omega = 0$; see Fig. 3 for an example.

The numbers L and a are shown in Fig. 4 for conditions along the $\Gamma^8\Theta^7 = 1$ line. Concordance of DFT results with known limits for $\Theta \ll 1$ ($L = \pi^2/3$ and $a = 0$), which are not susceptible to e-e scattering mechanisms due to Pauli blocking [11,65], had been established in the past [25,27].

However, in the opposite limit, Fig. 4 clearly shows that the DFT calculations do not approach the Spitzer results, but instead the Lorentz plasma values (e-i scattering only), which are substantially higher; see also Table I. Thus, we conclude that e-e collisions are not accounted for in DFT when following the KG formalism, i.e., by computing electronic transport coefficients from Eqs. (22).

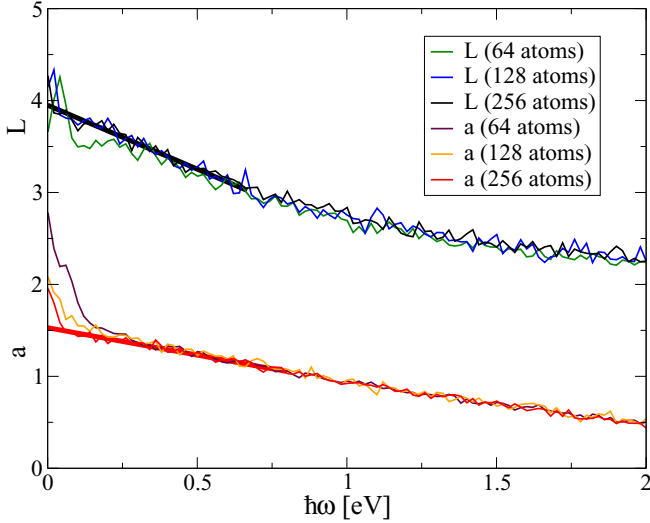


FIG. 3. Lorenz number and thermopower coefficient from our DFT calculations at 200 000 K and 0.3997 g/cm³ ($\Gamma = 0.84$ and $\Theta = 1.23$) for different particle numbers and their linear extrapolations (bold lines) to the DC limits.

VII. FURTHER DISCUSSION

The reason why e-e scattering is absent in DFT transport properties is that the Kohn-Sham interaction operator,

$$v_{KS}(\{\mathbf{r}_i\}) = \sum_i \left[- \sum_I \frac{e^2 Z_I}{4\pi \epsilon_0 |\mathbf{r}_i - \mathbf{R}_I|} + \frac{e^2}{4\pi \epsilon_0} \int d^3 \mathbf{r}' \frac{n_e(\mathbf{r}')}{|\mathbf{r}_i - \mathbf{r}'|} + v_{xc,i}(\mathbf{r}_i) \right], \quad (32)$$

where \mathbf{r}' is a position vector and \mathbf{r}_i and \mathbf{R}_I , respectively, are electronic and ionic position coordinates, has the same single-particle structure (separable into additive single-electron

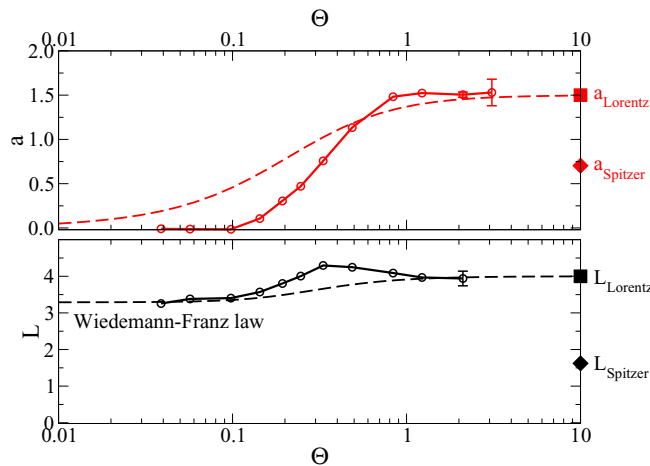


FIG. 4. Thermopower coefficient (red) and Lorenz number (black) from DFT (full) and RTA (dashed) along the $\Gamma^8 \Theta^7 = 1$ line.

TABLE I. Values for the transport coefficients for hydrogen plasma according to the Spitzer theory [3,49] accounting for e-i and e-e scattering compared with the values from the KG formalism (DFT) at $\Gamma = 0.52$ and $\Theta = 2.1$.

Quantity	Lorentz (e-i)	Spitzer (e-i and e-e)	DFT-MD
a	1.5	0.7033	1.51 ± 0.03
L	4.0	1.6220	3.94 ± 0.2

terms) as the interaction operator for adiabatic e-i scattering:

$$v_{ei}(\{\mathbf{r}_i\}) = - \sum_{i,I} \frac{e^2 Z_I}{4\pi \epsilon_0 |\mathbf{r}_i - \mathbf{R}_I|}, \quad (33)$$

but with the additional Hartree and exchange-correlation terms. To achieve the correct Spitzer results in a Hamiltonian-based formalism, which is possible within generalized linear response theory [21,22], e-e scattering has to be included directly via the fundamental two-particle interaction operator (not separable into additive single-electron terms):

$$v_{ee}(\{\mathbf{r}_i\}) = \sum_{i < j} \frac{e^2}{4\pi \epsilon_0 |\mathbf{r}_i - \mathbf{r}_j|}. \quad (34)$$

Such a treatment leads to mathematical structures that are significantly different from the compact set of Onsager coefficients (22) in the KG formalism [66,67]. The mean-field Hartree potential in DFT,

$$v_H(\{\mathbf{r}_i\}) = \sum_i \frac{e^2}{4\pi \epsilon_0} \int d^3 \mathbf{r}' \frac{n_e(\mathbf{r}')}{|\mathbf{r}_i - \mathbf{r}'|}, \quad (35)$$

which becomes merely a global constant in a homogeneous electron gas at very high T , is unable to reintroduce e-e collision effects in the electronic transport coefficients. The same applies to the exchange-correlation potential $\sum_i v_{xc,i}(\mathbf{r}_i)$, which vanishes $\sim T^{-1/2}$ according to the Debye-Hückel limiting laws [17] in a real plasma. Within the PBE approximation [56], which is used in our practical work, it reduces to a constant energy shift according the local density approximation [68,69] for a homogeneous electron gas at very high T and, thus, does not influence the velocity matrix elements either.

Electron-electron collisions, when taken into account explicitly in the theoretical description via kinetic theory [3] or generalized linear response theory [21–23], reshape the nonequilibrium momentum distribution of electrons [3]. Whether or not e-e collisions have a particular effect on the electronic heat current that is separable from the reshaping of the distribution function as suggested in Ref. [37] remains to be shown.

For additional comparison, Fig. 5 contains results from kinetic theory within the RTA from Sec. III. This model describes a Lorentz plasma of noninteracting electrons scattering randomly at ions with small momentum transfer (weak collisions). It is not able to capture the important influences of strong collisions, electronic correlations, and ionic structure present in DFT, which explains the deviations to the DFT conductivity. Because of the more difficult convergence of DFT conductivities compared to thermopower and Lorenz

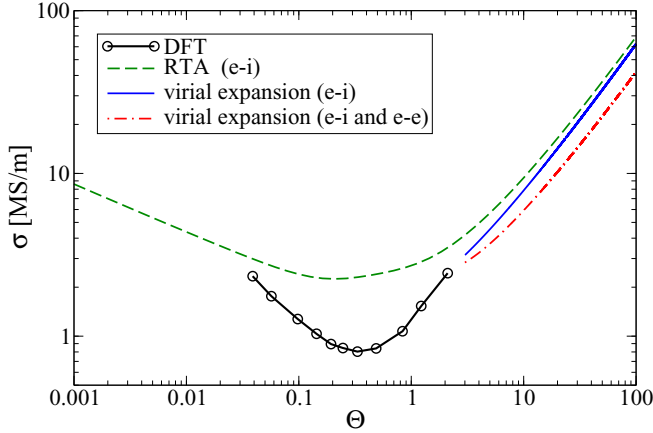


FIG. 5. Electrical conductivity from DFT, RTA, and the virial expansion with and without e-e collisions [39] as indicated in the legend along the $\Gamma^8\Theta^7 = 1$ line.

number, we cannot yet achieve an overlap between DFT and RTA data toward the nondegenerate limit.

To illustrate the influence of e-e scattering on the electrical conductivity, we also compare with results recently derived from the virial expansion in terms of Θ/Γ , which holds for $\Gamma/\Theta \ll 1$ and $\Theta \gg 1$, according to Ref. [39] (formulas are given in the Appendix B). The virial expansion accounts for dynamical screening effects and strong collisions and, probably due to the latter [70], approaches the DFT results better than the RTA model. The virial expansion can be elaborated for both Lorentz and Spitzer plasmas. In the latter case, the conductivity of the hydrogen plasma is smaller by a factor of 0.58 in the large- Θ limit [3,39].

On the one hand, the lack of e-e collisions may be a reason why DFT results have not yet been brought in accordance with conductivity models for dense, partially ionized plasmas more complex than fully ionized hydrogen [49]. On the other hand, DFT has certainly achieved great success in describing the electrical and thermal conductivity of liquid and solid metals like lithium [71], molybdenum [29], aluminum [26,34], and, with a caveat due to yet incomplete description of magnetism, also iron [28,35]. In light of our present findings, this implies that e-e scattering is of minor relevance at conditions in materials at geophysically relevant temperatures of few 1000 degrees K. This must not be confused with correlations between electrons, which certainly are important there and can approximately be captured by DFT.

Note that combining DFT with dynamical mean-field theory (DMFT) [72–75] allows for the introduction of additional electronic correlation effects beyond that of DFT, which also affect the electronic transport properties. However, these correlations are introduced artificially via localized repulsive interactions of certain electronic orbitals as offered by the Hubbard model and depend on external parameters that require additional constraints. Whether the DFT + DMFT method is potentially able to describe scattering between uncorrelated electrons via a proper Coulomb interaction $\sim 1/r$ is doubtful and has yet to be examined by an effort similar to ours, i.e., by benchmarking against the known limiting values for Spitzer and Lorentz plasmas.

While it is not obvious how e-e collisions can consistently be included into DFT approaches, a way to overcome these difficulties has been discussed in Ref. [37]. Within the generalized linear response theory [22,23,50,67], transport coefficients are expressed by higher-order correlation functions. Evaluating these with perturbation theory leads to renormalization factors that account for e-e collisions in relation to the Lorentz plasma model and depend on the degeneracy of the electron gas [36]. In the nondegenerate Spitzer limit [3], these renormalization factors are 0.5816 for L_0 , 0.2727 for L_1 , and 0.1970 for L_2 . Directly related to them are the renormalization factors 0.4689 for a and 0.4055 for L ; see also Table I. For strongly degenerate plasmas, all of these renormalization factors converge to 1.

Time-dependent DFT [76] seems an unlikely candidate for the introduction of e-e scattering because it is, like static DFT, a description of independent quasiparticles in an effective mean-field potential. It may, however, be able to describe effects from dynamical screening that are not included in static DFT calculations.

An alternative approach beyond DFT may be future development of quantum Monte Carlo techniques [77], which, however, require much higher computational effort than DFT. This applies especially to materials with multielectron atoms in realistic stoichiometry that many practical applications of WDM require, e.g., hydrogen-helium mixtures in Jupiter and Saturn [5,7,8] or iron-silicon-oxygen mixtures in Earth [78]. So far, quantitative predictions of transport properties of such systems can be made only with DFT-based methods.

VIII. CONCLUSION

In conclusion, we have resolved that electronic transport properties derived from DFT do not account for e-e collision effects. At present, DFT-MD simulations represent the most efficient and an indispensable approach to describe various properties of both condensed and warm dense matter. We have outlined directions for future developments to consistently include electron-electron collisions, including a promising combination of DFT with generalized linear response theory [21,22]. Our discussion indicates that such future efforts to develop transport theory [10] further can greatly benefit from systematic investigations of the Lorenz number and thermopower. Likewise, advancing experimental methods to determine thermopower and Lorenz number of warm dense matter will provide additional constraints to the theoretical methods aside from the Spitzer limiting values that the principal discussion of this article is tied to.

ACKNOWLEDGMENTS

We thank Heidi Reinholz for helpful discussions. M.F., M.S., and R.R. acknowledge support by the Deutsche Forschungsgemeinschaft (DFG) within the FOR 2440. The *ab initio* calculations were performed at the North-German Supercomputing Alliance (HLRN) facilities and at the IT and Media Center of the University of Rostock.

APPENDIX A: PAIR CORRELATION FUNCTION

The pair correlation function illustrated in Fig. 6 shows that protons are uncorrelated at 75 000 K and 0.6527 g/cm^3 and

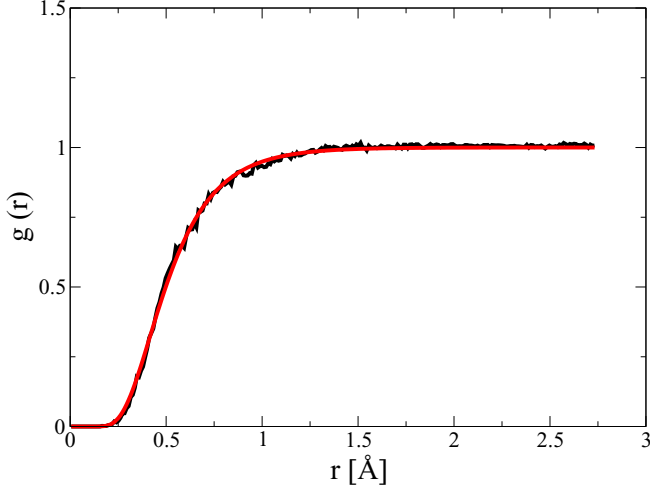


FIG. 6. Protonic pair correlation function from a DFT-MD simulation with 64 hydrogen atoms at 75 000 K and 0.6527 g/cm^3 (black line). Fit to a function $g(r) = \exp[-r_0 \exp(-kr)/r]$, where the fit parameters were determined as $r_0 = 2.259 \text{ \AA}$ and $\kappa = 3.77/\text{\AA}$ (red line).

are only subject to repulsive interactions at small distances r . A quantitative check of this observation is possible by fitting the pair correlation function to the expression [13]:

$$g(r) = \exp[-V(r)/k_B T], \quad (\text{A1})$$

which applies for uncorrelated particles interacting via a radial pair potential $V(r)$. The red line in Fig. 6 is the result of such a fit if a screened Coulomb potential for proton-proton interaction is assumed:

$$V(r) \sim \frac{\exp(-\kappa r)}{r}. \quad (\text{A2})$$

Using the same configurations of uncorrelated ions also at lower densities and higher temperatures by scaling the box

TABLE II. First and second virial coefficients for the conductivity of fully ionized hydrogen plasma with and without e-e scattering from Ref. [39].

Coefficient	Lorentz (e-i)	Spitzer (e-i and e-e)
ρ_1	$(2\pi^3)^{1/2}/16$	0.846
ρ_2	1.0	0.4917

size increases the distance between all ions further. This is sufficient to bring our system closer to the physical situation assumed in the derivation of the relevant high- T limiting cases for the transport properties, i.e., resistivity through uncorrelated collision events of electrons at individual scatterers [3].

APPENDIX B: VIRIAL EXPANSION FOR THE CONDUCTIVITY

Here we give the low-density limit of the electrical conductivity according to the virial expansion by Röpke *et al.* [39], which reads

$$\sigma [\text{S/m}] = \frac{32405.4 T_{\text{eV}}^{3/2}}{\rho_1 \ln(\Theta/\Gamma) + \rho_2 + \mathcal{O}[(\Gamma/\Theta)^{1/2} \ln(\Theta/\Gamma)]}, \quad (\text{B1})$$

with the virial coefficients as given in Table II. The virial expansion is valid for $\Gamma/\Theta \ll 1$ and $\Theta \gg 1$. For the plasma parameter Γ we have along the escape route $1/\Gamma = \Theta^{7/8}$. The temperature $T_{\text{eV}} = k_B T / \text{eV}$ in units of eV follows as

$$T_{\text{eV}} = 14.7761 \frac{1}{\Gamma^2 \Theta}. \quad (\text{B2})$$

Altogether, the virial expansion for σ along the escape route is given by

$$\sigma [\text{MS/m}] = \frac{1.84059 \Theta^{9/8}}{\frac{15}{8} \rho_1 \ln(\Theta) + \rho_2 + \mathcal{O}(\Theta^{-15/16} \ln \Theta)}. \quad (\text{B3})$$

- [1] L. Lorenz, *Ann. Phys. Chem.* **223**, 429 (1872).
 [2] J. M. Ziman, *Philos. Mag.* **6**, 1013 (1961).
 [3] L. Spitzer and R. Härm, *Phys. Rev.* **89**, 977 (1953).
 [4] T. Guillot, D. Gautier, G. Chabrier, and B. Mosser, *Icarus* **112**, 337 (1994).
 [5] A. Y. Potekhin, D. Baiko, P. Haensel, and D. G. Yakovlev, *Astron. Astrophys.* **346**, 345 (1999).
 [6] G. Schubert and K. M. Soderlund, *Phys. Earth Planet. Inter.* **187**, 92 (2011).
 [7] M. French, A. Becker, W. Lorenzen, N. Nettelmann, M. Bethkenhagen, J. Wicht, and R. Redmer, *Astrophys. J. Suppl. Series* **202**, 5 (2012).
 [8] R. Helled, *The Interiors of Jupiter and Saturn* (Oxford University Press, New York, NY, 2019).
 [9] J. Wicht, M. French, S. Stellmach, N. Nettelmann, T. Gastine, L. Duarte, and R. Redmer, in *Magnetic Fields in the Solar System*, Vol. 448 (Springer, Astrophysics and Space Science Library, Cham, 2018), pp. 7–82.
 [10] P. E. Grabowski, S. B. Hansen, M. S. Murillo, L. G. Stanton, F. R. Graziani, A. B. Zylstra, S. D. Baalrud, P. Arnault, A. D. Baczewski, L. X. Benedict, C. Blancard, O. Čertík, J. Clérouin, L. A. Collins, S. Copeland, A. A. Correa, J. Dai, J. Daligault, M. P. Desjarlais, M. W. C. Dharma-wardana *et al.*, *High Energy Density Phys.* **37**, 100905 (2020).
 [11] L. D. Landau and E. M. Lifshitz, *Physical Kinetics, Course of Theoretical Physics*, Vol. 10 (Pergamon Press, Oxford, 1981).
 [12] S. R. de Groot and P. Mazur, *Non-Equilibrium Thermodynamics* (Dover Publications, New York, 1984).
 [13] J. P. Hansen and I. R. McDonald, *Theory of Simple Liquids* (Academic Press, London, 1976).
 [14] J. A. McLennan, *Introduction to Non-Equilibrium Statistical Mechanics* (Prentice Hall, Englewood Cliffs, NJ, 1989).
 [15] M. Bonitz, *Quantum Kinetic Theory*, 2nd ed. (Springer, Cham, 2016).
 [16] W. Ebeling, V. E. Fortov, Y. L. Klimontovich, N. P. Kovalenko, W. D. Kraeft, Y. P. Krasny, D. Kremp, P. P. Kulik, V. A. Riaby,

- G. Röpke, E. K. Rozanov, and M. Schlanges, *Transport Properties of Dense Plasmas* (Akademie-Verlag, Berlin, 1984).
- [17] W.-D. Kraeft, D. Kremp, W. Ebeling, and G. Röpke, *Quantum Statistics of Charged Particle Systems* (Akademie-Verlag, Berlin, 1986).
- [18] R. Zimmermann, *Many-Particle Theory of Highly Excited Semiconductors* (Teubner Verlagsgesellschaft, Leipzig, 1988).
- [19] R. Kubo, *Rep. Prog. Phys.* **29**, 255 (1966).
- [20] R. Kubo, *J. Phys. Soc. Jpn.* **12**, 570 (1957).
- [21] D. Zubarev, V. Morozov, and G. Röpke, *Statistical Mechanics of Nonequilibrium Processes*, Vol. I (Akademie-Verlag, Berlin, 1996).
- [22] D. Zubarev, V. Morozov, and G. Röpke, *Statistical Mechanics of Nonequilibrium Processes*, Vol. II (Akademie-Verlag, Berlin, 1997).
- [23] H. Reinholz and G. Röpke, *Phys. Rev. E* **85**, 036401 (2012).
- [24] D. A. Greenwood, *Proc. Phys. Soc.* **71**, 585 (1958).
- [25] B. Holst, M. French, and R. Redmer, *Phys. Rev. B* **83**, 235120 (2011).
- [26] M. P. Desjarlais, J. D. Kress, and L. A. Collins, *Phys. Rev. E* **66**, 025401(R) (2002).
- [27] V. Recoules and J.-P. Crocombette, *Phys. Rev. B* **72**, 104202 (2005).
- [28] D. Alfè, M. Pozzo, and M. P. Desjarlais, *Phys. Rev. B* **85**, 024102 (2012).
- [29] M. French and T. R. Mattsson, *Phys. Rev. B* **90**, 165113 (2014).
- [30] N. de Koker, G. Steinle-Neumann, and V. Vlček, *Proc. Natl. Acad. Sci. U.S.A.* **109**, 4070 (2012).
- [31] M. Pozzo, C. Davies, D. Gubbins, and D. Alfè, *Nature (London)* **485**, 355 (2012).
- [32] D. V. Knyazev and P. R. Levashov, *Comput. Mater. Sci.* **79**, 817 (2013).
- [33] K. R. Cochrane, R. W. Lemke, Z. Riford, and J. H. Carpenter, *J. Appl. Phys.* **119**, 105902 (2016).
- [34] B. B. L. Witte, G. Röpke, P. Neumayer, M. French, P. Sperling, V. Recoules, S. H. Glenzer, and R. Redmer, *Phys. Rev. E* **99**, 047201 (2019).
- [35] J.-A. Korell, M. French, G. Steinle-Neumann, and R. Redmer, *Phys. Rev. Lett.* **122**, 086601 (2019).
- [36] H. Reinholz, G. Röpke, S. Rosmej, and R. Redmer, *Phys. Rev. E* **91**, 043105 (2015).
- [37] M. P. Desjarlais, C. R. Scullard, L. X. Benedict, H. D. Whitley, and R. Redmer, *Phys. Rev. E* **95**, 033203 (2017).
- [38] N. R. Shaffer and C. E. Starrett, *Phys. Rev. E* **101**, 053204 (2020).
- [39] G. Röpke, M. Schörner, R. Redmer, and M. Bethkenhagen, *Phys. Rev. E* **104**, 045204 (2021).
- [40] A. Lenard, *Ann. Phys.* **10**, 390 (1960).
- [41] R. Balescu, *Phys. Fluids* **3**, 52 (1960).
- [42] R. H. Williams and H. E. DeWitt, *Phys. Fluids* **12**, 2326 (1969).
- [43] R. A. Redmer, G. Röpke, F. Morales, and K. Kilimann, *Phys. Fluids B: Plasma Phys.* **2**, 390 (1990).
- [44] H. A. Lorentz, *Arch. Néerl.* **10**, 336 (1905).
- [45] S. Ichimaru, *Statistical Plasma Physics, Volume II: Condensed Plasmas* (Addison Wesley, Menlo Park, CA, 1994).
- [46] Y. T. Lee and R. M. More, *Phys. Fluids* **27**, 1273 (1984).
- [47] G. D. Mahan, *Many-Particle Physics*, edited by J. T. Devreese, R. P. Evrari, S. Lundqvist, G. D. Mahan, and N. H. March (Plenum Press, New York, 1981).
- [48] G. Röpke, *Theor. Math. Phys.* **194**, 74 (2018).
- [49] M. French and R. Redmer, *Phys. Plasmas* **24**, 092306 (2017).
- [50] G. Röpke, *Nonequilibrium Statistical Physics* (Wiley-VCH, Weinheim, 2013).
- [51] W. Kohn and L. J. Sham, *Phys. Rev.* **140**, A1133 (1965).
- [52] N. D. Mermin, *Phys. Rev.* **137**, A1441 (1965).
- [53] G. Kresse and J. Hafner, *Phys. Rev. B* **47**, 558 (1993).
- [54] G. Kresse and J. Hafner, *Phys. Rev. B* **48**, 13115 (1993).
- [55] G. Kresse and J. Furthmüller, *Phys. Rev. B* **54**, 11169 (1996).
- [56] J. P. Perdew, K. Burke, and M. Ernzerhof, *Phys. Rev. Lett.* **77**, 3865 (1996).
- [57] P. E. Blöchl, *Phys. Rev. B* **50**, 17953 (1994).
- [58] G. Kresse and D. Joubert, *Phys. Rev. B* **59**, 1758 (1999).
- [59] A. Baldereschi, *Phys. Rev. B* **7**, 5212 (1973).
- [60] S. Nosé, *J. Chem. Phys.* **81**, 511 (1984).
- [61] W. G. Hoover, *Phys. Rev. A* **31**, 1695 (1985).
- [62] H. J. Monkhorst and J. D. Pack, *Phys. Rev. B* **13**, 5188 (1976).
- [63] M. Gajdoš, K. Hummer, G. Kresse, J. Furthmüller, and F. Bechstedt, *Phys. Rev. B* **73**, 045112 (2006).
- [64] The phenomenological equations in Ref. [25] are misprinted.
- [65] A. Sommerfeld and H. Bethe, *Elektronentheorie der Metalle* (Springer, Berlin, 1967).
- [66] H. Reinholz, R. Redmer, and D. Tamme, *Contrib. Plasma Phys.* **29**, 395 (1989).
- [67] R. Redmer, *Phys. Rep.* **282**, 35 (1997).
- [68] D. M. Ceperley and B. J. Alder, *Phys. Rev. Lett.* **45**, 566 (1980).
- [69] J. P. Perdew and A. Zunger, *Phys. Rev. B* **23**, 5048 (1981).
- [70] Dynamical screening effects are not included in static DFT calculations.
- [71] A. Kietzmann, R. Redmer, M. P. Desjarlais, and T. R. Mattsson, *Phys. Rev. Lett.* **101**, 070401 (2008).
- [72] L. V. Pourovskii, J. Mravlje, A. Georges, S. I. Simak, and I. A. Abrikosov, *New J. Phys.* **19**, 073022 (2017).
- [73] J. Xu, P. Zhang, K. Haule, J. Minar, S. Wimmer, H. Ebert, and R. E. Cohen, *Phys. Rev. Lett.* **121**, 096601 (2018).
- [74] Y. Zhang, M. Hou, G. Liu, C. Zhang, V. B. Prakapenka, E. Greenberg, Y. Fei, R. E. Cohen, and J.-F. Lin, *Phys. Rev. Lett.* **125**, 078501 (2020).
- [75] L. V. Pourovskii, J. Mravlje, M. Pozzo, and Alfè, *Nat. Commun.* **11**, 4105 (2020).
- [76] E. Runge and E. K. U. Gross, *Phys. Rev. Lett.* **52**, 997 (1984).
- [77] F. Lin, M. A. Morales, K. T. Delaney, C. Pierleoni, R. M. Martin, and D. M. Ceperley, *Phys. Rev. Lett.* **103**, 256401 (2009).
- [78] M. Pozzo, C. Davies, D. Gubbins, and D. Alfè, *Phys. Rev. B* **87**, 014110 (2013).